# High silica concentration in RO concentrate

Haidari, A. H.; Witkamp, G. J.; Heijman, S. G.J.

**DOI**
10.1016/j.wri.2022.100171

**Publication date**
2022

**Document Version**
Final published version

**Published in**
Water Resources and Industry

**Citation (APA)**
Haidari, A. H., Witkamp, G. J., & Heijman, S. G. J. (2022). High silica concentration in RO concentrate. *Water Resources and Industry*, *27*, Article 100171. https://doi.org/10.1016/j.wri.2022.100171

Water Resources and Industry 27 (2022) 100171

Contents lists available at ScienceDirect

Water Resources and Industry

journal homepage: www.elsevier.com/locate/wri

# High silica concentration in RO concentrate

A.H. Haidari [a,*], G.J. Witkamp [b], S.G.J. Heijman [c]

[a] Hatenboer-water, Mercuriusweg 8, 3113 AR, Schiedam, the Netherlands
[b] King Abdullah University of Science and Technology (KAUST), Water Desalination and Reuse Center (WDRC), Division of Biological and Environmental Science and Engineering (BESE), Thuwal, 23955-6900, Saudi Arabia
[c] Delft University of Technology, Faculty of Civil Engineering, Stevinweg 01, 2628 CN, Delft, the Netherlands

ARTICLE INFO

*Keywords:*
Membrane fouling
Reverse osmosis
Silica scaling
PHREEQC

ABSTRACT

Silica scaling is one of the major scaling challenges in Reverse Osmosis (RO). The safe operation practice is to keep the silica concentration below 150 mg/L in RO concentrate. This study addresses the effects of divalent cations such as calcium and magnesium on silica scaling in a seawater RO installation used as a pretreatment to Eutectic Freeze Crystallisation (EFC). Results showed that in the absence of antiscalant and divalent cations a sustained silica concentration of approximately 280 mg/L in concentrate is possible without declining membrane permeability. At a higher concentration of divalent cations, the membrane permeability decreased. Membrane autopsy and analysing destructed membrane showed a relatively low magnesium and a high calcium concentration on the membrane after adding divalent ions into the solutions. It is concluded that in absence of divalent cations and without antiscalant the limits of 150 mg/L silica can be extended to 280 mg/L for 6–8 h.

## 1. Introduction

Safe and clean water is in short supply across the globe. Reverse osmosis (RO) offers a solution to the water shortage because it offers an excellent barrier against source water constituents. Depending on the type of water that is to be treated, RO can be categorised in sanitary RO, brackish water RO (BWRO), and seawater RO (SWRO). Sanitary RO is typically used to treat waters with a salinity under 1000 mg/L TDS (total dissolved solids), BWRO for waters with salinities between 1000 and 12000 mg/L TDS, and SWRO for waters with salinity higher than 12,000 mg/L TDS. This makes sanitary RO suitable for treatment of fresh water or tap water, BWRO for treatment of brackish groundwater, and SWRO for treatment of seawater, concentrate of BWRO or concentrate of SWRO [1,2]. For instance, application of BWRO in green houses widely occurs in many countries where horticulture is an economic pillar, such as the Netherlands. In the western part of the Netherlands, about 30% of required water for horticulture is provided by BWRO using brackish ground water. It is predicated that in the coming years the usage of BWRO will increase due to significant and rapid climate change, and population increase. This increases the necessity of finding techno-economic solutions to (i) reduce the membrane scaling, which is the main fouling mechanism in BWRO, and (ii) to prevent environmental damages that can occur as a consequence of discharging concentrate into the ground by inland installations [3].

Concentrate disposal is the most significant environmental consideration for inland BWRO facilities. Common methods for handling RO concentrate include discharge to surface water, discharge to the sewage system, using an evaporation pond, evaporation,

---

* Corresponding author.
*E-mail address:* amir.haidari@brabantwater.nl (A.H. Haidari).

https://doi.org/10.1016/j.wri.2022.100171
Received 22 September 2021; Received in revised form 14 January 2022; Accepted 22 January 2022

**Nomenclature and abbreviations**

| *Chemical formula* | *Name* |
|---|---|
| Ca | Calcium |
| Mg | Magnesium |
| Si | Silicon |
| Br | Bromide |
| Cl | Chloride |
| K | Potassium |
| Na | Sodium |
| Fe | Iron |
| Mn | Manganese |
| $PO_4^{2-}$ | Phosphate |
| $SO_4^{2-}$ | Sulphate |
| $SiO_2$ | Silica |
| $CaCO_3$ | Aragonite |
| $BaSO_4$ | Barite |
| $CaCO_3$ | Calcite |
| $SiO_2$ | Chalcedony |
| $Mg_3Si_2O_5(OH)_4$ | Chrysotile |
| $CaMg(CO_3)_2$ | Dolomite |
| $Ca_5(PO_4)_3OH$ | Hydroxyapatite |
| $SiO_2$ | Quartz |
| $Mg_2Si_3O_7 \cdot 5OH:3H_2O$ | Sepiolite |
| $Mg_3Si_4O_{10}(OH)_2$ | Talc |

| *Abbreviation* | |
|---|---|
| TCF | Temperature correction factor for water viscosity |
| EFC | Eutectic freeze crystallisation |
| RO | Reverse osmosis |
| CCRO | Closed-circuit reverse osmosis |
| MTC | Mass (in this study water) transfer coefficient |
| Jw | Water flux |
| NDP | Net driving pressure |
| Qp | Permeate flow |
| EC | Electrical conductivity |
| – | pH |
| T | Temperature |
| $T_{act}$ | Actual temperature |
| $T_{ref}$ | Reference temperature |
| $P_f$ | Feed pressure |
| $P_c$ | Concentrate pressure |
| $P_p$ | Permeate pressure |
| $\pi_f$ | Osmotic pressure in feed |
| $\pi_p$ | Osmotic pressure in permeate |
| $\pi_c$ | Osmotic pressure in concentrate |
| $A_{mem}$ | Effective area of membrane |

eutectic freeze crystallisation (EFC) and deep well injection [4]. Choosing the proper method to deal with concentrate depends on the concentrate quality, site location characteristics, system recovery, available facilities at the location, and local regulations. Evaporation ponds provide an economic solution for concentrate treatment in hot, arid areas with inexpensive land available. In this method, concentrate is pumped into large ponds and water slowly evaporates via direct solar energy. The simplicity of this process reduces maintenance and operating costs and reduces energy input [5]. In addition, the produced salt can be used in industry. The evaporation ponds are normally constructed in the remote area to reduce the effects of possible pollution transferred by the wind.

Deep well injection is frequently used to dispose the concentrate by inland sites. In this method, concentrate is injected down a deep well into a confined aquifer which is not connected to any adjacent fresh or brackish water aquifers [4,6]. However, the environmental regulations are becoming stricter using deep well injection as a result of the unknown effects of concentrate on the target aquifer. One of the measures to reduce these unknown effects is to avoid dosing of antiscalant. However, this limits the recovery of BWRO to 50% or less and increases the energy consumption for producing the same amount of water.

Evaporation and/or EFC is recommended for concentrate treatment when treatment methods such as evaporation ponds and deep well injection are not feasible. These techniques consume vast amounts of energy, and in order to be economically efficient need pretreatment processes to minimise the volume and maximise the salt concentration of their feed. To prepare the BWRO concentrate as feed for these techniques, the installation has to work at the highest possible recovery and (or alternatively) thicken the concentrate before these techniques using SWRO. Furthermore, when SWRO is applied, the highest possible recovery is desirable in order to reduce the concentrate treatment costs. To increase the efficiency of these techniques and obtain products (salts) of a high purity, no antiscalant should be added into the water during the RO process(es).

As the recovery rate increases, the magnitude of concentration polarisation increases, and membrane scaling can occur. Undesirable consequences of scaling include a decline in membrane flux (water production), deterioration in product water quality by increased salt passage or increased operating pressure to maintain flux with a subsequent increase in energy costs.

Scaling is the primary fouling mechanism in BWRO operating at high recovery and treatment of its concentrate. Biofouling and particulate fouling are less important in BWRO because of the anaerobic conditions of groundwater (in most cases), natural and artificial screens before the RO, and the fact that groundwater is directly fed to the BWRO installations in aerobic conditions. The absence of microorganisms and particles in the feed water of BWRO results in the absence of these substances in the concentrate. Thus, reducing the concentrate volume depends on the concentration of dissolved ions, types of ions present in concentrate, type of membrane, and operational conditions.

The current research provides experimental data on the silica scaling in SWRO when used for reducing the concentrate volume of BWRO and preparing it as the feed to the EFC/evaporator for optimal efficiency. That is interesting because typically silica is not considered a compound of high scaling in SWRO because (i) seawater contains silica of less than 20 mg/L with an average of 4–5 mg/L [1,5] (ii) typical recovery of SWRO installation is rather low (about 30–50%).

## 2. Background

Silica can be found in many different forms and it is influenced by a variety of factors including temperature, pH, metal ions such as strontium, potassium, sodium, aluminium, and iron, and ionic strength [7,8]. The soluble form of silica is initially monomeric, as it contains only one silicon atom [9], and is called monosilicic acid.

The silica dissolution involves a chemical reaction or hydrolysis in an excess of water [10]:

$$SiO_2 + 2H_2O \rightarrow Si(OH)_4 \tag{1}$$

Many studies are performed on the silica solubility in water at temperatures between 0 and 100 °C. A solubility of 70 mg/L is reported for anhydrous nonporous amorphous silica at 25 °C, and a solubility of 100–140 mg/L for the common forms of silica [10]. Kempter et al. [8] reported a solubility of 6 mg/L for crystalline silica and 180 mg/L for amorphous silica.

Monosilicic acid, which is a weak acid, remains in the monomeric state for long periods in water at 25 °C as long as the concentration is below 2 mM (around 300 mg/L), but usually polymerises rapidly at higher concentrations due to the condensation reaction [10–12]. It polymerises by dehydration to form Si–O–Si anhydride bonds (dimer from) and, as a result, respectively dimers (two subunits linked) and oligomers (a finite number of subunits linked) are formed [13]. Finally, colloidal polymers and particulate silica will be formed. The dimerisation reaction is shown below.

$$Si(OH)_4 + OH^- \rightarrow SiO(OH)_3{}^- + H_2O \tag{2}$$

$$SiO(OH)_3{}^- + Si(OH)_4 \rightarrow (OH)_3SiOSi(OH)_3 + OH^-[Dimerization] \tag{3}$$

In the literature it is shown that each type of membrane reacts differently with silica. RO is typically suitable for removing dissolved silica and ultrafiltration for colloidal silica. Depending on whether the polymerisation of silica occurs on the interface (surface) of the membrane or in the bulk solution, the silica fouling can be classified into respectively precipitation fouling or scaling and particulate fouling. Scaling occurs when monomeric silica polymerises at the membrane surface, and therefore scaling is enhanced by a high rejection of dissolved silica by the RO membrane. Particulate fouling of silica occurs as a result of silica colloids accumulating after they are formed in the bulk solution and at the membrane surface. Therefore, ultrafiltration is typically used to remove non-reactive silica.

Because removing silica scaling from RO membrane surface is not possible with current cleaning mechanisms and without damaging the membrane, it is preferred to prevent silica scaling. The conventional method to control silica scaling system is by operating the RO system at low recovery and limiting the silica concentration to less than 150 mg/l as $SiO_2$ [14]. The industrial guideline suggests a maximum concentration of 120 mg/l as $SiO_2$ in the concentrate flow at 25 °C [14]. By dosing of a dedicated antiscalant against silica scaling, the system can operate with a silica concentration up to 300 [mg/l $SiO_2$] [8,15,16]. However, dosing antiscalant reduces the purity of salts produced by EFC/evaporators when these techniques are applied to treat the RO concentrate with an ensuing decrease in the salts value.

Moreover, the pressure retarded osmosis process is more susceptible for silica scaling. Wang et al. [16] reported that silica scaling during the pressure retarded osmosis process can occur at a concentration as low as 10 mg/L. They found that the precipitation and deposition of silica mainly occurred at the interface between the rejection layer and the support layer. They showed that low pH using an acidic draw solution can be an effective method for silica scaling control.

The scaling mechanism of silica remains difficult to understand. Kempter et al. [17] investigated the adsorption and the formation of silica scale on RO-membrane surfaces by means of time-resolved atomic force microscopy. Results show that the first step of silica precipitation without additives is the formation of colloidal particles in the range of 20–30 nm in the bulk solution which deposit onto the membrane surface. Over time, the surface is densely covered with $SiO_2$ particles. Tong et al. [18] investigated the relationship between membrane surface properties and silica scaling in RO. They showed that the rate of silica scaling was independent of both the membrane hydrophilicity and the free energy for heterogeneous nucleation, but depended on the membrane surface charge. Their results show that positively charged membranes significantly facilitated silica scaling, whereas a more negative membrane surface charge leads to reduced scaling.

Tong et al. [18] suggested that deposition of positive species on the membrane can enhance silica scaling. This finding is confirmed by Sheikholeslami et al. [9]. They state that the formation kinetics of polymeric silica from monosilic acid is catalysed by hydroxide ions, accelerated by the presence of salts such as CaCl2 and MgCl2, and influenced by the pH. Calcium can stimulate the formation of filterable silica (size >0.45 μm) in low concentration silica solution and magnesium can stimulate the formation of filterable silica polymers in high silica concentration [19,20].

Presence of other ions such as aluminium in feed water of RO can also enhance the silica scaling. The use of aluminium sulphate (alum) coagulation prior to reverse osmosis (RO) was investigated by Gabelich et al. [21]. They showed that the coagulation process with alum causes membrane fouling. This resulted from the reaction of soluble aluminium with ambient silica ($H_4SiO_2$) and forming kaolinite within the RO unit. Lunevich et al. [22] explain that the presence of aluminium on silicate species has three effects: (i) aluminium ions connected to silicate, (ii) aluminium ions forced rearrangement of species into smaller groups, and (iii) it is likely that some silicate species precipitated as aluminium silicate. Their study also suggests that sodium ions prevent silica deposition on the membrane surface.

While the presence of aluminium is of high importance for the formation of silica scaling, it is not considered in this study since the original water used in this experiment was groundwater in which no aluminium was detected. Most naturally occurring aluminium compounds have very low solubility between pH 6 and 9. Therefore, dissolved forms rarely occur in natural waters in concentrations exceeding 0.01 mg/L [23].

Compared to aluminium, there is a higher chance that calcium and magnesium occurring in groundwater together with silica. Typically, hardness scaling (mainly calcium and magnesium) is considered reversible whereas silica and silicate scaling as irreversible. Silica scaling, in the light form, can be removed from the membrane by using ammonium bifluoride, but redissolving silica in the severe form will damage the membrane [15,24]. When both the hardness ions and silica are present in water, silica scaling can be enhanced. Koo et al. [12] found that an increase in calcium and magnesium concentration resulted in the increase of the polymerisation rate of silica. Sheikholeslami [9] et al. reported that the Ca/Mg ratio did not affect the solubility limit of the silica but influences the rate of polymerisation.

Separate measures should be taken to prevent or reduce the scale formation of salts formed due to the hardness ions or silica. Kempter et al. [17] showed that within 24 h experiment virtually no polymerisation occurs up to 400 mg/L initial silica in hard water (28° German hardness), temperature of 40 °C, pH 7, and without any additives. Above the supersaturation level of 400 mg/L, an immediate precipitation occurs. In RO systems operating at pH above 9, hydroxide of cations such as calcium, magnesium, strontium, potassium, and sodium are capable of undergoing reaction with silica [14,25]. Among the resulting products, magnesium silicate scaling ($MgSiO_3$) is more likely to scale the membrane, which is dense, and strenuous to be removed [26]. Although commonly referred to as $MgSiO_3$, magnesium silicate is hypothesised to be present in water treatment systems as a result of a multistep process resulting in a mixture of a variety of chemical species containing magnesium and silica [14]. The first step is the formation of magnesium hydroxide ($Mg[OH]_2$). The hydroxide salt reacts with monomeric silicate anion and/or polymeric silica to form magnesium silicate [26].

The formation of silica scaling species can be mitigated by removing silica ions or the hardness ions from the feed water of RO. Silica removal techniques include dosing lime, or dosing coagulants such as aluminium or iron, electrocoagulation, adsorption, ion exchange, and seeded precipitation [27]. However, the most common pretreatment method in water and wastewater treatment is to

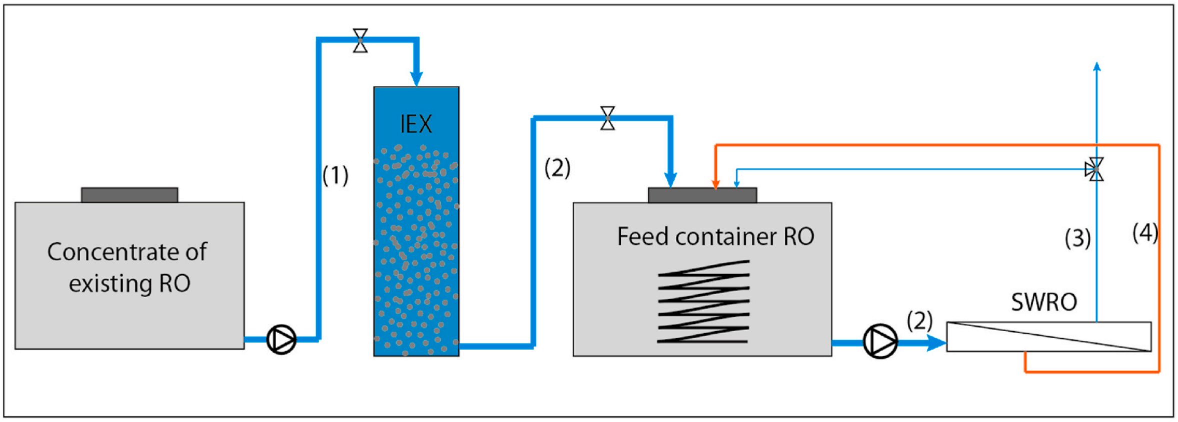

**Fig. 1.** Experimental setup. Concentrate of the current RO passed through a cation ion exchange column (IEX). The produced softened water by IEX was used as the feed to RO in the experimental setup. During the operation at constant feed composition, permeate and concentrate are recirculated back into the feed container. During the concentration mode, the permeate was discharged into the sewage. **Flows:** (1): Concentrate of existing RO = effluent of IEX, (2): effluent of IEX = feed to RO in experimental setup, (3): permeate of RO, (4): concentrate of RO.

apply ion exchange softeners to remove hardness ions and pH-increase to alleviate silica scaling. Additionally, it is possible to reduce the pH and consequently risks of calcium and magnesium scaling.

The literature only reveals limited information regarding the effects of calcium and magnesium on silica scaling in RO without using antiscalant, particularly in combination with ion exchange softeners.

The current study aims to investigate the scaling potentials of the RO installation at a high silica concentration without using antiscalant, and in the absence of divalent hardness cations. To this aim, the concentrate from a BWRO installation, which was directly applied on groundwater, is collected, passed through an ion exchange column, and fed to a SWRO. In addition, the effects of increasing the concentration of calcium and magnesium on the formation of silica complexes are investigated. This is performed by stepwise increase of the concentration factor of the feed water of the SWRO. This study contributes to an efficient treatment of industrial brine containing silica, magnesium, and calcium as well as understanding the role of hardness ions in initiation of silica scaling in SWRO.

## 3. Material and methods

Fig. 1 shows a schematic view of the experimental setup. The concentrate of an existing BWRO system (1) was passed through a cation Ion Exchange column (IEX) filled with Amberlite-IRC747 (Dupont) resins to remove multivalent cations such as $Ca^{2+}$ and $Mg^{2+}$ and $Fe^{3+}$. The effluent of IEX was collected in a tank, after which it was fed to SWRO (SWC2540 from Hydranautics) as a means to decrease its volume and prepare it to be used by the EFC unit.

The concentrate was collected on the same day in six IBC tanks of each 1000L from a brackish groundwater RO system operating at recovery of around 50% without adding any antiscalant. An IEX column filled with Amberlite-IRC747 was used to remove the hardness ions from the concentrate. Amberlite-IRC747 resin has a macroporous structure. Its polystyrenic matrix, cross-linked with divinylbenzene, contains amino-phosphonic groups. The chemical nature of these groups is such that they form complexes with metal ions. According to the manufacturer, this resin features high operating capacity for calcium, and is especially useful when treating brine. The softened effluent of IEX (2) entered a 3 $m^3$ container and was used as the feed water for the RO in the setup. SWC2540 from Hydranautics was used to thicken the effluent of IEX. SWC2540 is an SWRO membrane and made of composite polyamide membrane with a minimum slat rejection of 99%. At pH 7, the membrane zeta potential is −21.2 mV [28]. The initiation of scaling was predicted by measuring the mass transfer coefficient (MTC) at a constant flux (15 $L/h.m^2$) and a constant element recovery (8%).

Three experiments were performed during which the parameters for determining the membrane's MTC were measured at a specific feed concentration and in several steps for a period of about 8 h. To maintain constant feed composition during this 8-h trajectory, permeate and concentrate streams of RO were recirculated back into the feed tank while the temperature was kept constant using a cooling spiral. After the constant feed composition process, permeate was discharged and the feed solution was allowed to build up a higher concentration. Next, the experiment was continued with a new concentration (Fig. 2).

The solution diffusion model, one of the theories that describe the transport of mass through the RO membranes, describes the performance of a perfect, non-defected membrane. At given conditions, the membrane MTC remains constant until fouling occurs, i.e.,

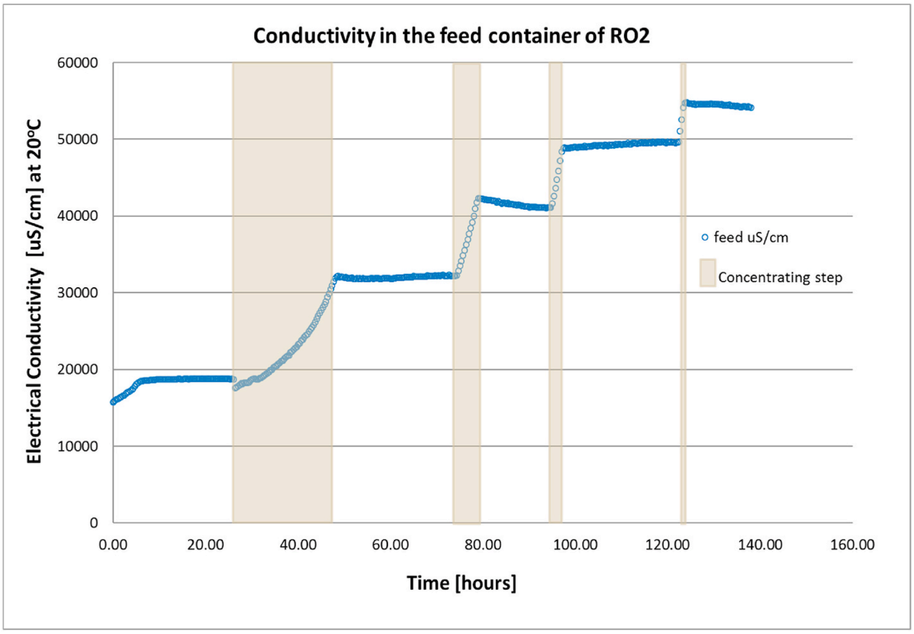

**Fig. 2.** Two modes were used during each experiment: constant feed composition mode and concentrating mode. During the constant feed composition mode, the permeate and concentrate were recirculated back into the feed tank to keep the feed composition constant and during the concentrating mode, the permeate is discharged to increase the concentration of ions in the solution.

MTC indicates the membrane permeability for water. MTC is based on the membrane characteristics such as the thickness and porosity, and can be estimated by using Equation (4) [16,29]. $J_w$ is the water flux, $Q_p$ is the permeate flow, $A_{mem}$ is effective membrane area, MTC is the membrane mass transfer coefficient, TCF is temperature correction factor, and NDP is net driving pressure [30].

$$MTC = \frac{Q_p \times TCF}{A_{mem} \times NDP} \tag{4}$$

In the solution diffusion model, the transport of solute and solvent are independent of each other. The flux of solvent through the membrane is linearly proportional to the effective pressure difference across the membrane.

$$J_w = \frac{Q_p}{A_{mem}} = \frac{MTC \times NDP}{TCF} \tag{5}$$

NDP is a measure of available driving pressure to force the water from the feed-concentrate channel to the permeate channel. Thus, NDP is the difference between the transmembrane pressure ($\Delta P$) and the transmembrane osmotic pressure ($\Delta\pi$) [29].

$$NDP = \Delta P - \Delta\pi = \left(\frac{P_f + P_c}{2} - P_p\right) - \left(\frac{\pi_f + \pi_c}{2} - \pi_p\right) \tag{6}$$

Osmotic pressures are calculated using electrical conductivity instead of actual concentration of ions. To this end, the temperature correction and two conversion factors are used; one empirical conversion factor is used to convert the electrical conductivity to the Total Dissolved Solids (TDS), and another one is used for the conversion of TDS to the osmotic pressure (Equation (7)) [30].

$$\pi = EC \times factor\ (EC \rightarrow TDS) \times factor\ (TDS \rightarrow \pi) \times \left(\frac{273 + T_{act}}{273 + T_{ref}}\right) \tag{7}$$

Before each experiment, the system was operated with demineralised water for about 24 h to recover the initial MTC. Membrane cleaning and operating of membrane at constant conditions (feed concentration, temperature, and flux) ensure that MTC changes only with the membrane fouling, i.e., in the given conditions MTC can be used as an indicator of membrane fouling.

Table 1 represents the effluent of cationic IEX, i.e., the initial feed concentration in each experiment. The initial conditions (Table 1) are not exactly the same in all experiments because the IEX capacity decreases in time. Consequently, the value of $Ca^{2+}$ and $Mg^{2+}$ concentration is lowest in experiment 01 and highest in experiment 03. It can be seen that during the concentration mode, the concentration of all ions including calcium and magnesium increases.

Additionally, we inspect the membrane visually, destructed the membrane and analysed the results, and used a model to investigate the reason of MTC decrease; whether it is because of membrane fouling, and to determine the nature of fouling. The visual inspection is performed with the electronic microscope. Since the visual inspection does not reveal any information about the nature of fouling, two equal-sized membrane pieces from different locations are cut and destructed. Thereafter their elemental ions are determined and compared. Information from the destruction method gives only local information about the detected ions found, but not about the type of scaling. Therefore, a geochemical model, PHREEQC, is used to calculate the saturation indexes. The saturation indexes are used to make a prediction about the type of scaling on the membrane surface. More detailed explanation about the methods used in this study can be found in the results and discussion section.

## 4. Results and discussion

### 4.1. Permeate water

No divalent ions or silica were detected in the RO permeate. The salinity of permeate increased at the higher thickening factors. The highest measured EC in permeate was 1380 µS/cm. That is mainly caused by the presence of sodium, chlorite, and species of inorganic

**Table 1**
Concentration of the feed water of the experiment (concentrate of a brackish water RO treated with IEX).

| Description | Unit | Experiment 1 | Experiment 2 | Experiment 3 |
|---|---|---|---|---|
| EC | µS/cm | 16,300 | 16,230 | 15,200 |
| pH | – | 8.9 | 7.6 | 6.8 |
| T | °C | 21.0 | 20.7 | 21.7 |
| $SiO_2$ | mg/L | 47 | 53 | 60 |
| $Br^-$ | mg/L | 17 | 19 | 18 |
| $Ca^{2+}$ | mg/L | 0.43 | 7 | 50 |
| $Cl^-$ | mg/L | 6216 | 5400 | 6027 |
| $K^+$ | mg/L | 97 | 119 | Not measured |
| $Mg^{2+}$ | mg/L | 0.16 | 29 | 74 |
| $Na^+$ | mg/L | 4027 | 3158 | 3322 |
| $Fe^{3+}$ | mg/L | <0.1 | <0.1 | <0.1 |
| $Mn^{3+}$ | mg/L | <0.1 | <0.1 | <0.1 |
| $PO_4^{2-}$ | mg/L | 7.44 | 4 | 0.76 |
| $SO_4^{2-}$ | mg/L | 2 | 2 | 2 |

carbon.

### 4.2. MTC

MTC can be used as an indication tool for determining the initiation of membrane fouling. To determine the initiation of membrane fouling, we performed experiments with SWRO and used the obtained results to calculate the MTC. The calculated MTC's are presented in Fig. 3, Fig. 4, and Fig. 5. The initial water composition for each experiment is mentioned in Table 1.

MTC starts at different values in each figure (Figs. 3, Fig. 4, and Fig. 5), because of the different thickening factor of feed solution in the recirculation mode. As explained, MTC is calculated using the measured EC of solution, which is caused by an inaccurate calculation of the osmotic pressure. However, during each recirculation mode the salt concentration remains constant and therefore the osmotic pressure in each recirculation mode remains the same. This means that if no fouling occurs, the MTC in each recirculation mode should not change, i.e., a straight horizontal MTC line indicates no fouling and/or scaling.

Figs. 3 and 4 show that the MTC decline was not significant up to thickening factor five (CF = 3.5) indicating that no detectable fouling or scaling occurred in experiment 1 and experiment 2. These graphs show a slight decrease of MTC at higher thickening factor.

Contrary to experiment 1 and 2, Fig. 5 shows a rapid decrease of MTC at CF = 3.5 in experiment 3.

Fig. 6 compares the MTC of three membranes. The graph shows that the MTC decreases due to the increase in concentration of calcium and magnesium. While not significant, there is an MTC-decrease in experiment 02 compared to experiment 01. The MTC decrease becomes remarkable in experiment 03 when the concentration of calcium and magnesium are respectively 50 and 74 mg/L in the initial state. The decrease of MTC indicates the initiation of membrane fouling. By a continued membrane process, scaling of membrane occurs. Discontinued processes such as closed-circuit reverse osmosis (CCRO) [31,32] can offer a solution to postpone the scaling. This type of process can further reduce the concentrate volume further until it meets the criteria needed in order for it to be treated by the final processes such as EFC and evaporation.

At the given conditions, the MTC decrease is typically the result of membrane fouling. To have visual evidence if the membrane is fouled, autopsy was performed on each membrane. First, the unravelled membrane is scanned with the naked eye, then, the suspected parts (to fouling) are identified, and finally, are inspected under an electron microscope. Fig. 7 shows a very small part of the membrane (L = 65 μm x b = 50 μm) under the electron microscope. The figure shows that the diameter of the largest observed fouling spot was about 15 μm.

The nature of the fouling/scaling could not be determined, neither by the MTC figures (Figs. 3, Fig. 4, and Fig. 5) nor by the observation of fouling under the microscope (Fig. 7). Therefore, two pieces of membrane (b = 10 cm by h = 10 cm) from the element in experiment 03 were destructed by hydrofluoric (HF) in the laboratory and under standard protocols (ASTM D6357). Table 2 shows the concentration of elements achieved form destructing the membrane coupon. Coupon 01 was obtained from a part of membrane that seemed to be fouled and Coupon 02 from a part which seemed glassy compared to other parts of the membrane.

The results from Table 2 show that respectively sulphur, silicon and calcium have the highest concentration. The high sulphur (s)

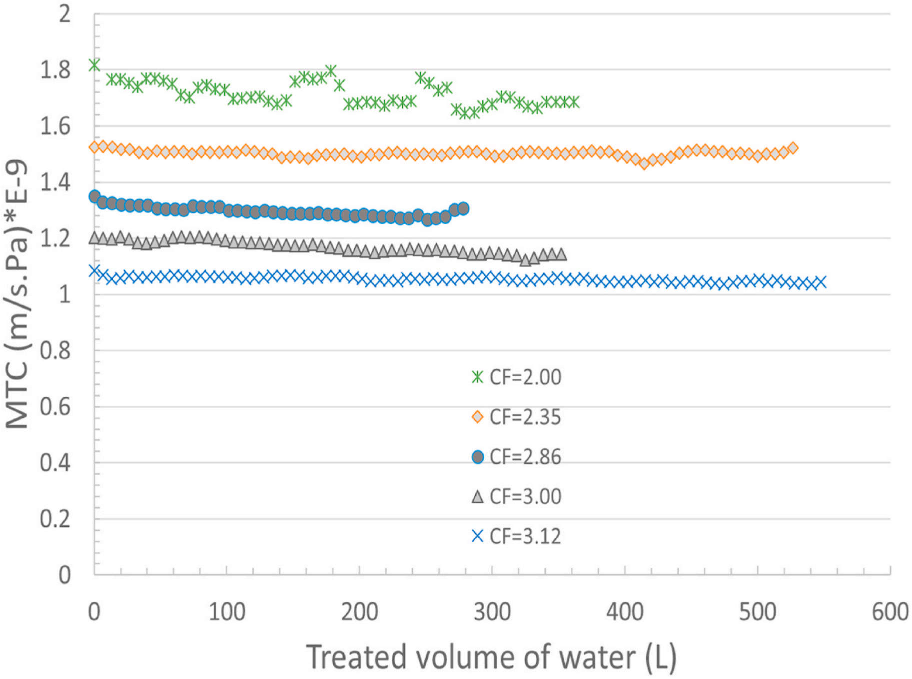

**Fig. 3.** Mass transfer coefficient (MTC) with an initial $Ca^{2+}$ and $Mg^{2+}$ concentration of less than 1 mg/L ($Mg^{2+}/Ca^{2+} = 0.4$) (Experiment 01).

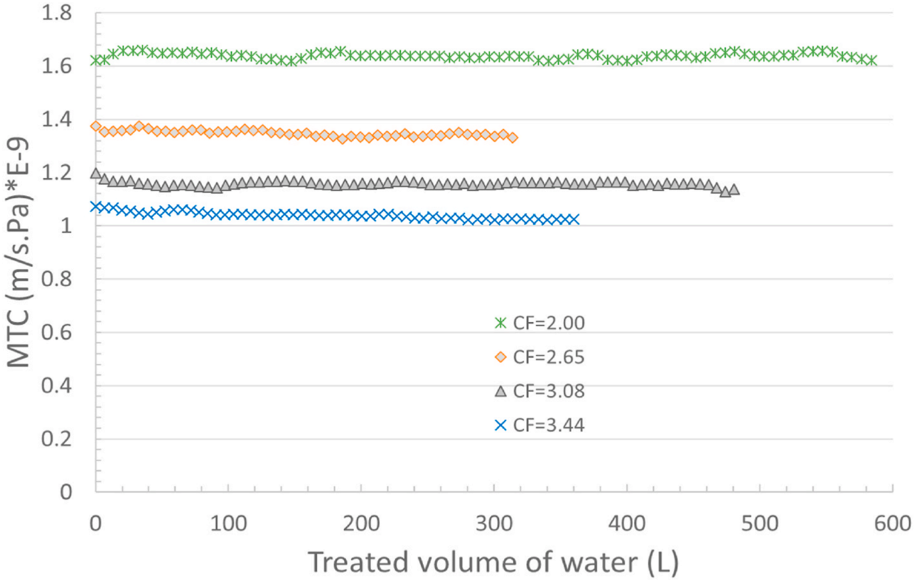

**Fig. 4.** Mass transfer coefficient (MTC) with a $Ca^{2+}$ concentration of 7.5 mg/L and a $Mg^{2+}$ concentration of 29 mg/L ($Mg^{2+}/Ca^{2+} = 4$) (Experiment 02).

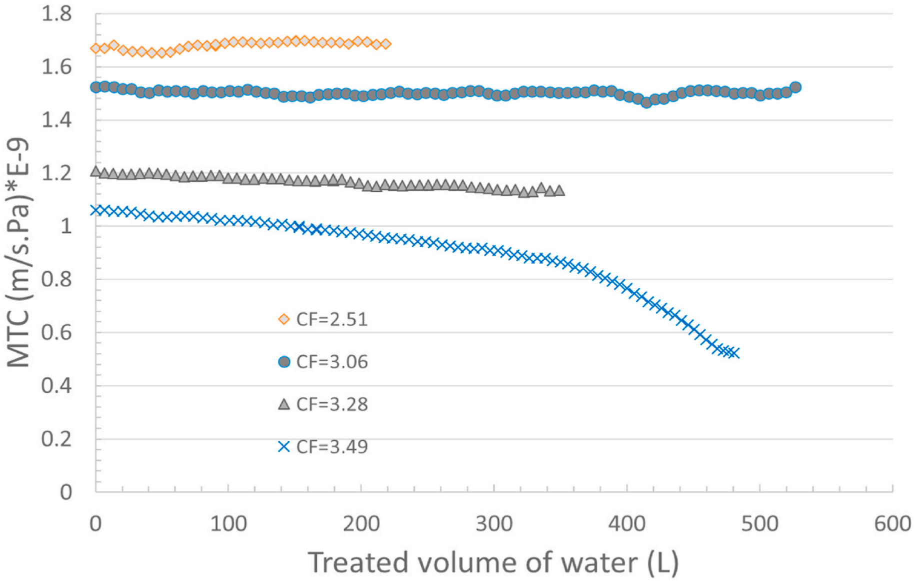

**Fig. 5.** Mass transfer coefficient (MTC) with a $Ca^{2+}$ concentration of 50 mg/L and a $Mg^{2+}$ concentration of 75 mg/L ($Mg^{2+}/Ca^{2+} = 1.5$) (Experiment 03).

concentration is originated from the membrane material itself because the support layer of most polyamide membrane is made of polysulphide. Expectedly, the concentration of silica in Coupon 02 (with a glassy part inside) is higher than Coupon 01. This is an indication of the local silica scaling on the membrane. The higher calcium concentration in Coupon 01 could be an indication of local calcium precipitation.

In another attempt to determine the type of fouling, PHREEQC is used to detect which substances could cause the MTC declination. PHREEQC is a computer program designed to perform a wide variety of aqueous geochemical calculations and processes in natural waters or laboratory experiments [33]. It has different database models, one of which has to be used based on the input data and purpose of the modelling. One of these databases called “PhreeqC”, which uses ion-association and Debye Hückel expressions to account for the non-ideality of the aqueous solutions. This type of aqueous model is adequate at low ionic strength but may break down at higher ionic strengths (in the range of seawater and above). In sodium chloride dominated systems, such as this study, the PhreeqC database is reliable at higher ionic strengths [34].

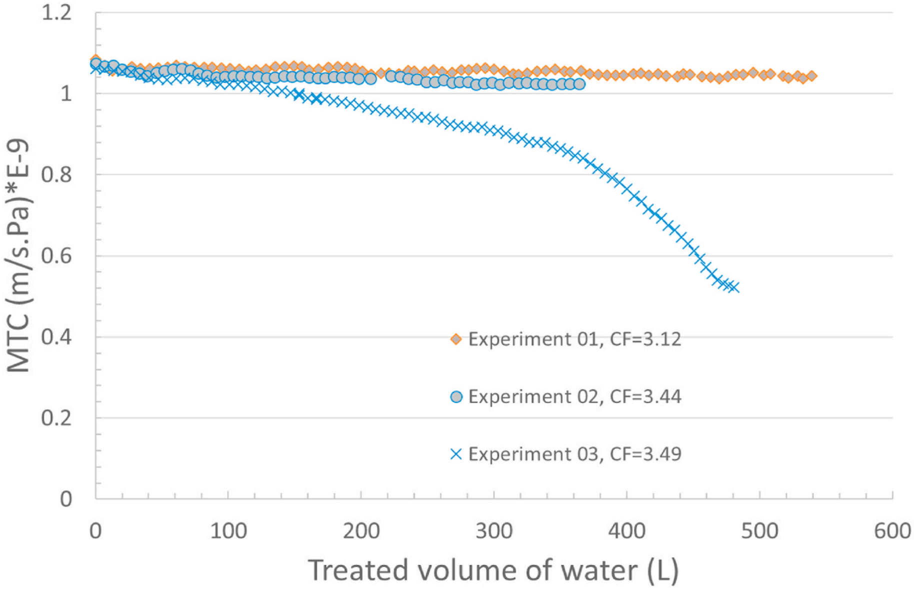

**Fig. 6.** Mass transfer coefficient (MTC) in experiment 01 with initial $Ca^{2+}$ concentration = 0.43 mg/L and $Mg^{2+}$ concentration = 0.16 mg/L, experiment 02 with initial $Ca^{2+}$ concentration = 7 mg/L and $Mg^{2+}$ concentration = 29 mg/L and experiment 03 with initial $Ca^{2+}$ concentration = 50 mg/L and $Mg^{2+}$ concentration = 74 mg/L.

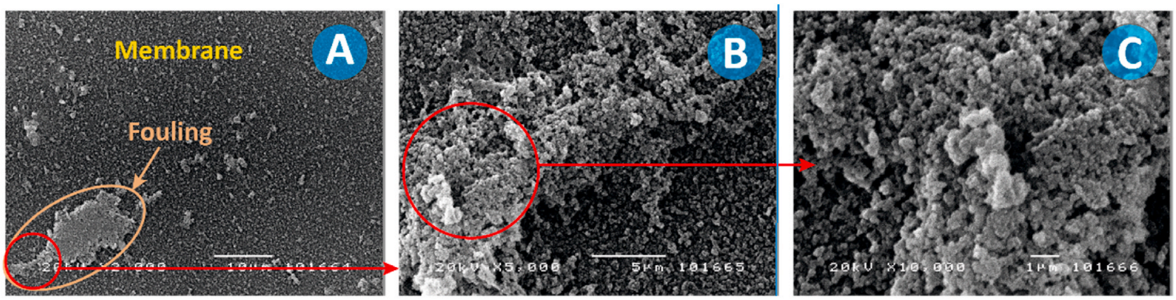

**Fig. 7.** Small part of membrane where the fouling was visible observed at different magnitude (A = x2000, B = x5000 and C = x10000) under an electron microscope.

**Table 2**
Detected elements from destruction of the membrane coupons.

| Chemical element | Symbol | Amount [μg/$cm^2$] | |
|---|---|---|---|
| | | Coupon 01 | Coupon 02 |
| Barium | Ba | <0.05 | <0.05 |
| iron | Fe | 0.41 | 0.73 |
| copper | Cu | 0.66 | 0.13 |
| molybdenum | Mo | <0.05 | <0.05 |
| zinc | Zn | 0.28 | 1.3 |
| Silicon (Silica) | Si | 28 (60) | 100 (214.29) |
| Calcium | Ca | 1.7 | 0.061 |
| Magnesium | Mg | 0.09 | 0.12 |
| Phosphor | P | <0.05 | <0.05 |
| Sulphur | S | 140 | 110 |

Table 3 shows the input values for the PHREEQC simulation, which is a dataset of four samples from the RO concentrate in experiment 03 at concentration factors 1, 2.51, 3.06, 3.28 and 3.49. The temperature and pH used for simulation are measured during the experiments while the ion concentration is analysed with ion chromatography (IC) after the experiments. Most of the ions are more concentrated after a concentration step. But the increase is lower than expected from the concentration factor. The reason for these lower values is twofold: ions are not rejected 100% by the membrane and pass to the permeate side of the membrane. This is mainly the case at higher concentrations and for monovalent ions. The other reason is that ions are transformed into the solid precipitate. The PHREEQC output includes different parameters among which saturation index (SI) that determines, which scaling can be formed on the membrane.

Fig. 8 illustrates the SI variations by increasing the concentration factor. For the ease of visibility, salts with low saturation index are removed from Fig. 8. Based on the results from Fig. 8, three important groups of species could be distinguished.

(1) species that have only silica molecules in their chemical formulations such as chalcedony, quartz and silicic acid ($SiO_2$(a)). The SI value of this group increases by increasing the CF up to CF = 3.28 and then decreases by further increase.
(2) Species with magnesium and silica in their chemical formulation such as sepiolite and talc. The SI values of this group show a fast increase with the increase of the CF. In the last concentration step, the SI does not further increase indicating the start of scaling. This is confirmed by the results found by Amjad et al. [26]. They found that among hydroxides of cations, the magnesium silicate scaling (MgSiO3) is more likely to scale the membrane and more strenuous to be removed when precipitated because of their dense structure.

It is observed that talc has a very high supersaturation, but the SI increases with each concentration step. Only the last concentration step shows a constant SI indicating that the ions for this salt are no longer accumulating and scaling occurs. This agrees with the MTC-decrease at the highest concentration of experiment 03.

Furthermore, the SI of seplolite does not further increase at the last concentration step. So also, this silica component will be scaling in this experiment.

(3) It appears that, no calcium-silica precipitates were formed during the experiment. However, dolomite which is composed of the calcium, magnesium, and carbonate is a possible scaling component.

## 5. Conclusions

The main aim of this study was to determine the effects of calcium and magnesium in silica scaling of reverse osmosis (RO). The effects of other ions such as aluminium and iron are not considered in this study. This is mainly because the original groundwater did not contain aluminium. The concentration of iron approximated 3 mg/L in this water which was reduced to <0.1 mg/L after the IEX and virtually zero before the SWRO. In fact, in the absence of any antiscalant, no membrane mass transfer (MTC) decrease was observed up to a silica concentration of 280 mg $SiO_2$/L at low concentration of calcium and magnesium, indicating no membrane fouling. This is, of course, only valid for the timeframe where each experiment is conducted (about 8 h).

Increasing the calcium and magnesium concentration resulted in the decline of mass transfer coefficient (MTC) by the membrane.

Analysing different membrane coupons from the experiment with a sudden decrease in MTC showed a high concentration of silica on some parts of the membrane and calcium on the other parts. Simulation with PHREEQC software and results from membrane destruction pointed out that the formation potential of magnesium-silica species is higher than calcium-silica species at the given conditions and confirmed the findings of previous studies. However, the related mechanisms should be more widely investigated. The

**Table 3**
The input data used for PHREEQC. The samples are collected during the third experiment at different thickening factors (CF = 1, 2.51, 3.06, 3.28 and 3.49).

| Description | | | Sample Name | | | | |
|---|---|---|---|---|---|---|---|
| Name | Symbol | Unit | Sample CF1 | Sample CF3.1 | Sample CF4 | Sample CF4.6 | Sample CF5 |
| Concentration factor based on EC | TF | – | 1 | 2.51 | 3.06 | 3.28 | 3.49 |
| pH | pH | – | 7.5 | 7.5 | 7.6 | 7.9 | 7.9 |
| Average Temperature | T | ºC | 20.9 | 22.3 | 22.4 | 22.9 | 23.3 |
| Boron | B | mg/L | 0.97 | 1.46 | 1.52 | 1.60 | 1.62 |
| Barium | Ba | mg/L | 0.12 | 0.12 | 0.20 | 0.21 | 0.21 |
| Bromine | Br | mg/L | 18.2 | 32.3 | 35.3 | 37 | 37.5 |
| Calcium | Ca | mg/L | 50.2 | 22.2 | 42.3 | 29 | 25.5 |
| Copper | Cu | mg/L | 0.06 | 1.59 | 0.34 | 0.47 | 0.5 |
| Potassium | K | mg/L | 118 | 216 | 226 | 245 | 249 |
| Lithium | Li | mg/L | 0.24 | 0.62 | 0.61 | 0.70 | 0.73 |
| Magnesium | Mg | mg/L | 73.5 | 160 | 164 | 151 | 141 |
| Manganese | Mn | mg/L | 0.07 | 0.07 | 0.12 | 0.12 | 0.11 |
| Phosphate | $PO_4$ | mg/L | 0.76 | 2.64 | 1.28 | 1.34 | 1.30 |
| Sulphate | $SO_4$ | mg/L | 2.13 | 11.7 | 25.6 | 29 | 29.2 |
| Strontium | Sr | mg/L | 4.93 | 6.53 | 10.8 | 12 | 11.6 |
| Zinc | Zn | mg/L | 0.08 | 0.15 | 0.10 | 0.05 | 0.05 |
| Silicon | Si | mg/L | 27.3 | 48.9 | 75.6 | 58 | 53.8 |
| Inorganic Carbon | C | mg/L | 900 | 886 | 750 | 713 | 721 |
| Sodium | Na | mg/L | 3322 | 7526 | 7946 | 9462 | 10,044 |
| Chloride | Cl | mg/L | 6027 | 13,656 | 15,460 | 18,631 | 19,858 |

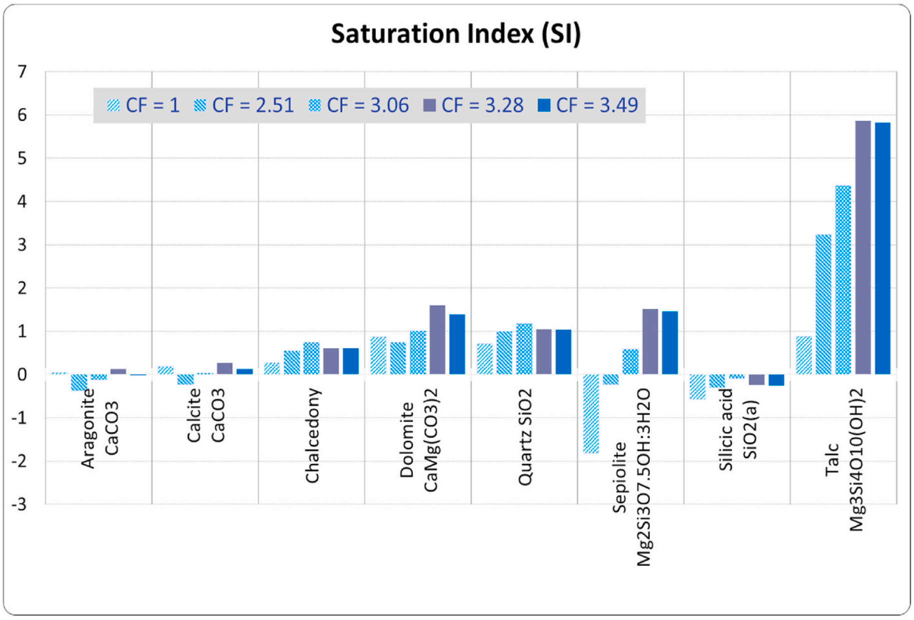

**Fig. 8.** SI (saturation index) value of possible precipitated substances in feed water reservoir at different thickening factors.

current study reveals that silica scaling can be enhanced by magnesium ions, probably by talc and/or sepiolite formation, under conditions similar to those in this study. It is probably helpful to use the closed-circuit reverse osmosis (CCRO) techniques instead of continued (conventional) RO to reduce the concentrate volume without enhancing silica scaling. Using of CCRO is the topic of our next study related to silica.

Our forthcoming follow-up study related to silica addresses the use of the closed-circuit reverse osmosis (CCRO) techniques instead of continued (conventional) RO to reduce the concentrate volume without enhancing silica scaling. We also advise further investigating the effect of other ions in the water matrix such as sodium, chloride, iron, and aluminium.

## Author statement

A.H. Haidari: Writing the article and performing the experiments/rewriting the article/making changes and uploading the article. S.G.J. Heijman: Critical review of results and mentoring/revision of the article. G.J. Witkamp: Global consideration of results and initial review of the article/revision of the article/providing assets.

## Declaration of competing interest

The authors declare that they have no known competing financial interests or personal relationships that could have appeared to influence the work reported in this paper.

## Acknowledgements

We would like to thank Hatenboer-Water for their support and providing RO-equipment for the experiments and ZERO BRINE (Horizon 2020 project with grant number 730390) for their support for writing this article.

## References

[1] V. Nikolay, Desalination Engineering: Planning and Design, McGraw-Hill Professional, 2012.
[2] J. Kucera, Reverse Osmosis Industrial Processes and Applications, 2015.
[3] A.H. Haidari, B. Blankert, H. Timmer, S.G.J. Heijman, W.G.J. van der Meer, PURO: A Unique RO-Design for Brackish Groundwater Treatment, (Desalination).
[4] P.O.J.M. Ian C, P.E. Watson Jr., Lisa Henthorne, PE DESALTING HANDBOOK for PLANNERS, Bureau of Reclamation Denver Federal Center, 2003, p. 316.
[5] B. Ladewig, B. Asquith, Evaporation ponds, in: Desalination Concentrate Management, Springer Berlin Heidelberg, Berlin, Heidelberg, 2012, pp. 49–57.
[6] N. Voutchkov, G.N. Kaiser, Chapter 6 - deep well injection, in: N. Voutchkov, G.N. Kaiser (Eds.), Management of Concentrate from Desalination Plants, Elsevier, 2020, pp. 137–149.
[7] R.Y. Ning, Arsenic removal by reverse osmosis, Desalination 143 (2002) 237–241.
[8] S.D.N. Freeman, R.J. Majerle, Silica fouling revisited, Desalination 103 (1995) 113–115.
[9] R. Sheikholeslami, S. Tan, Effects of water quality on silica fouling of desalination plants, Desalination 126 (1999) 267–280.
[10] R.K. Iler, I.R. K, The Chemistry of Silica: Solubility, Polymerization, Colloid and Surface Properties and Biochemistry of Silica, Wiley, 1979.
[11] R.Y. Ning, Discussion of silica speciation, fouling, control and maximum reduction, Desalination 151 (2003) 67–73.
[12] T. Koo, Y.J. Lee, R. Sheikholeslami, Silica fouling and cleaning of reverse osmosis membranes, Desalination 139 (2001) 43–56.

[13] R. Sheikholeslami, I.S. Al-Mutaz, S. Tan, S.D. Tan, Some aspects of silica polymerization and fouling and its pretreatment by sodium aluminate, lime and soda ash, Desalination 150 (2002) 85–92.
[14] C.W. Smith, Pilot test results utilizing polymeric dispersants for control of silica, in: Z. Amjad (Ed.), Water Soluble Polymers: Solutions Properties and Applications, Springer US, Boston, MA, 2002, pp. 173–182.
[15] I. Bremere, M. Kennedy, S. Mhyio, A. Jaljuli, G.-J. Witkamp, J. Schippers, Prevention of silica scale in membrane systems: removal of monomer and polymer silica, Desalination 132 (2000) 89–100.
[16] J.S. Gill, Inhibition of silica—silicate deposit in industrial waters, Colloids Surf. A Physicochem. Eng. Asp. 74 (1993) 101–106.
[17] A. Kempter, T. Gaedt, V. Boyko, S. Nied, K. Hirsch, New insights into silica scaling on RO-membranes, Desalination Water Treat. 51 (2013) 899–907.
[18] T. Tong, S. Zhao, C. Boo, S.M. Hashmi, M. Elimelech, Relating Silica Scaling in Reverse Osmosis to 5 Membrane Surface Properties 6 7 8 9, Environmental Science & Technology, 2017.
[19] G. Braun, W. Hater, C.z. Kolk, C. Dupoiron, T. Harrer, T. Götz, Investigations of silica scaling on reverse osmosis membranes, Desalination 250 (2010) 982–984.
[20] J.D. Hem, G. Survey, Study and Interpretation of the Chemical Characteristics of Natural Water, Department of the Interior, U.S. Geological Survey, 1985.
[21] C.J. Gabelich, W.R. Chen, T.I. Yun, B.M. Coffey, I.H. Mel Suffet, The role of dissolved aluminum in silica chemistry for membrane processes, Desalination 180 (2005) 307–319.
[22] L. Lunevich, P. Sanciolo, A. Smallridge, S.R. Gray, Silica scale formation and effect of sodium and aluminium ions -29Si NMR study, Environ. Sci. Water Res. Technol. 2 (2016) 174–185.
[23] E.R. Weiner, Applications of Environmental Aquatic Chemistry : a Practical Guide, 2013.
[24] W. Byrne, Reverse Osmosis: A Practical Guide for Industrial Users, Tall Oaks Pub., 1995.
[25] S.Q.A. Mahat, I.M. Saaid, B. Lal, Green silica scale inhibitors for Alkaline-Surfactant-Polymer flooding: a review, J. Petrol. Explor. Prod. Technol. 6 (2016) 379–385.
[26] Z. Amjad, S. American Chemical, C. Division of, C. Surface, S. American Chemical, P. Meeting, Symposium on Water Soluble Polymers: Solution, Applications, Water Soluble Polymers : Solution Properties and Applications, 1998.
[27] N.A. Milne, T. O'Reilly, P. Sanciolo, E. Ostarcevic, M. Beighton, K. Taylor, M. Mullett, A.J. Tarquin, S.R. Gray, Chemistry of silica scale mitigation for RO desalination with particular reference to remote operations, Water Res. 65 (2014) 107–133.
[28] C. Conidi, F. Macedonio, A. Ali, A. Cassano, A. Criscuoli, A. Pietro, E. Drioli, Treatment of flue gas desulfurization wastewater by an integrated membrane-based process for approaching zero liquid discharge, Membranes 8 (2018) 117.
[29] A.H. Haidari, S.G.J. Heijman, W.G.J. van der Meer, Optimal design of spacers in reverse osmosis, Separ. Purif. Technol. 192 (2018) 441–456.
[30] H. Huiting, M. de Koning, E.F. Beerendonk, in: Nieuwegein KIWA (Ed.), Normalisatie van gegevens bij nanofiltratie en omgekeerde osmose, September 1999.
[31] A. Efraty, CCD series no-16: opened vs. closed circuit SWRO batch desalination for volume reduction of Silica containing effluents under super-saturation conditions, Desalination Water Treat. 57 (2016) 9569–9584.
[32] A. Efraty, R.N. Barak, Z. Gal, Closed circuit desalination — a new low energy high recovery technology without energy recovery, Desalination Water Treat. 31 (2011) 95–101.
[33] D. Parkhurst, T. Appelo, User's Guide to PHREEQC Version 3 - a Computer Program for Speciation, Batch-Reaction, One-Dimensional Transport, and Inverse Geochemical Calculations, 1999.
[34] D.L. Parkhurst, C.A.J. Appelo, User's guide to PHREEQC (Version 2) : a computer program for speciation, batch-reaction, one-dimensional transport, and inverse geochemical calculations, in: Water-Resources Investigations Report, 1999.